2021 International Siberian Conference on Control and Communications (SIBCON) | 978-1-7281-8504-0/20/$31.00 ©2021 IEEE | DOI: 10.1109/SIBCON50419.2021.9438910

Ultrasound sensor modeling in Gazebo simulator for diagnostics of abdomen pathologies

Bulat Abbyasov*, Alexandra Dobrokvashina*, Roman Lavrenov*, Enzhe Kharisova†, Tatyana Tsoy*, Liliya Gavrilova*, Sergey Bulatov†, Elena Maslak‡, Natalia Schiefermeier-Mach§ and Evgeni Magid*
*Laboratory of Intelligent Robotic Systems (LIRS)
Intelligent Robotics Department
Institute of Information Technology and Intelligent Systems
Kazan Federal University
Kazan, Russia
abbyasov@it.kfu.ru, dobrokvashina@it.kfu.ru, lavrenov@it.kfu.ru, tt@it.kfu.ru, liliya@it.kfu.ru, magid@it.kfu.ru
†Center of a practical skills
Kazan State Medical University
Kazan, Russia
cardiorean@mail.ru, boulatov@rambler.ru
‡Department of Industrial Engineering and Manufacturing
Volgograd State Medical University
Volgograd, Russia
eemaslak@yandex.ru
§Health University of Applied Sciences
Innsbruck, Austria
natalia.schiefermeier-mach@fhg-tirol.ac.at

***Abstract*—Ultrasound imaging is a widely used technique in medicine. It is a non-invasive medical procedure that uses sound waves to produce pictures of the inside of the human body. Ultrasound helps to diagnose conditions of soft tissues and detecting a wide range of medical diseases and pathologies. This paper presents a 3D model and a Gazebo plugin of a medical ultrasound sensor that performs ultrasound imaging of an abdomen surface. The ultrasound device is represented as an end-effector for a KUKA IIWA LBR manipulator model but can also be used for other manipulator models. We introduce an implementation of a complex abdomen 3D model that consists of fat, muscle, and intestine tissue layers. Each tissue has its unique parameters used by the Gazebo medical ultrasound plugin. The developed ultrasound sensor was successfully tested in the Gazebo simulator and was able to provide visualizing a structure of the abdomen internals for further diagnostics.**

***Index Terms*—medical robotics, Gazebo, ROS, medical ultrasound sensor, non-invasive surgery**

I. Introduction

Over the last two decades, robot-assisted procedures have become popular in many surgical scenarios [1], [2]. Medical robotics is used in various aspects of medicine - from surgical intervention and palpation to therapy and rehabilitation [3]. Medical robotic systems allow surgeons to perform various procedures safer and quicker with clinically supported precision and accuracy [4]. At present, surgical robots have been successfully applied in minimally invasive surgery such as pelvic organ prolapse, defects and other basin basement reconstruction operations [5]. For example, the versatile robots for assistance tasks in the surgery field are the da Vinci Surgical System [6] and KUKA LBR Med [7].

There is also another surgery method - a non-invasive approach. This kind of surgery techniques is a conservative treatment that does not require inclusion into the body or removal of tissue [8], [9]. It is based on non-ionizing radiation, so it does not have the same risks as X-rays or other types of imaging systems that use ionizing radiation. Palpation, visualizing abdominal tissues and organs, assessing bone fragility, heat therapy, listening to the fetal heart beat, and blood pressure measurements are non-invasive medical procedures.

The most frequently used application of non-invasive techniques is ultrasonography [10]. It is a diagnostic imaging method applied in therapeutic tasks to produce an image of internal body structures: muscles, blood vessels, etc. Ultrasound images are captured in real-time using special devices called transducers. A transducer is placed directly on the skin. A thin layer of gel is applied to the skin so that ultrasound waves are transmitted through the gel into the body. Perhaps the most well-known application of ultrasound is monitoring a pregnancy. Ultrasound provides the ability to view an image of a fetus as it develops inside the mother's womb. While this is an important use, there are many other applications of ultrasound in medicine. From diagnostic testing to treating cancer, tumors, and other serious pathologies, ultrasound transducers play a key role in today's healthcare [11].

Acquisition of optimal images is greatly dependent on sonographer skill [12]. A sonographer must manipulate a transducer through various angles and may need to apply significant forces to obtain quality images and can make a wrong diagnosis [13]. However, there are places where a skilled sonographer may not be available. For example, in small clinics and rural areas where patients have difficulties in accessing medical services [14]. Several medical robotic ultrasound imaging systems have been proposed [15]–[17]. However, to the best of our knowledge, medical robotic ultrasound imaging system modeling and simulation are not covered thoroughly in present researches.

This paper describes a software package for ultrasound sensor modeling in the Gazebo simulator. The package allows simulating ultrasound imaging process using a special Gazebo plugin. For imitating medical conditions we developed an abdomen 3D model formed by layers of tissues: fat, muscle, and intestine. Each tissue has its unique parameters used by the Gazebo medical ultrasound plugin. KUKA IIWA LBR was selected as a manipulator model. The developed ultrasound sensor was successfully tested by simulating abdominal ultrasound imaging and was able to provide visualizing the abdomen internals.

II. Ultrasound sensor architecture

The developed software package is a complex ROS-based package, which consists of several components that interact with ROS/Gazebo ecosystem [18]. An architecture of the ultrasound sensor is shown in Fig. 1. The package is divided into four main parts:

- **Gazebo plugin** is responsible for parsing abdomen tissue parameters, processing background logic and mathematics of ultrasound imaging, and producing ultrasound images.
- **Medical ultrasound transducer** is a 3D model model representing an experimental prototype of an ultrasound device. The ultrasound device can easily be modified and further attached to other manipulator models.
- **Multi-layer abdomen model** is a complex 3D model of an abdominal wall. The abdominal wall is modeled as a multi-layer medium including skin, fat, muscle, and intestine, where each layer has its thickness, density, propagation speed and texture.
- **Manipulator control node** includes point cloud processing from a Kinect depth camera, poses generation, and motion planning for moving the manipulator to a new position.

A process flow of simulating the ultrasound sensor is shown in Fig. 2.

At first, the ultrasound transducer should be attached to an arbitrary robotic manipulator model. It could be done by modifying a URDF file that describes all elements of the manipulator robot model: links, joints, materials, inertial, etc [19]. The modification requires only including a special XML extension file to the URDF file and specifying the name of the manipulator link where the device will be added.

The second step is creating a virtual simulation environment. The package yet contains a ready-to-use Gazebo medical procedure simulation world file including a surgical table, the Kinect camera, and the configured abdomen model. Model and link structures are well-documented, and a user can easily and quickly customize all model parameters and add new configurations.

The extension *ultrasound_sensor_plugin* is responsible for reading and processing abdomen tissue information. It expands a World file by incorporating special model descriptions. The package module allows setting a structure of tissues for further parsing by the Gazebo system extended with our developed plugin.

We used the manipulator control module proposed by Shafikov et al. [20]. In order to comply the ultrasound imaging procedure, module components were redesigned. The depth map is acquired by subscribing "/kinect_depth_map" and filtered by a point cloud processing module using Point Cloud Library (PCL) [21]. The poses generation and motion planning modules use different abdomen examination patterns applied in ultrasonography.

III. Simulation setup

A. Virtual environment

Simulation environment in the Gazebo (Fig. 3) contains the modified KUKA IIWA LBR manipulator model [22]. KUKA IIWA LBR is placed on a cubic supporting base that shifts the workspace in order to cover surgical table surface. The Kinect camera model with a Robot Operating System (ROS) depth camera plugin is mounted on a tripod to enable palpated surface geometry data acquisition. A human abdomen model is placed on the surgical table within the manipulator workspace and the Kinect camera range. To model ultrasound influence KUKA IIWA LBR is equipped with a transducer device (Fig. 4).

B. Medical ultrasound imaging system

The typical medical ultrasonic imaging system consists of an ultrasonic transducer and an imaging system. The imaging system controls the ultrasonic transducer in order to transmit and receive the ultrasound, and creates an ultrasound image using a set of data from the transducer.

Gazebo simulator does not provide any internal functionalities and API to simulate the realistic ultrasound beam emission behavior in the simulation. The available ultrasound sonar sensor can only compute an approximated distance to the simulation object by colliding a cone with objects in the world. The closest collision point is used to compute the range returned by the sonar. The main issue that the real wave should transmit itself through the tissue mediums. Ultrasound rays implemented in Gazebo get only the range value to the first link of the model and do not take into account the following link layers.

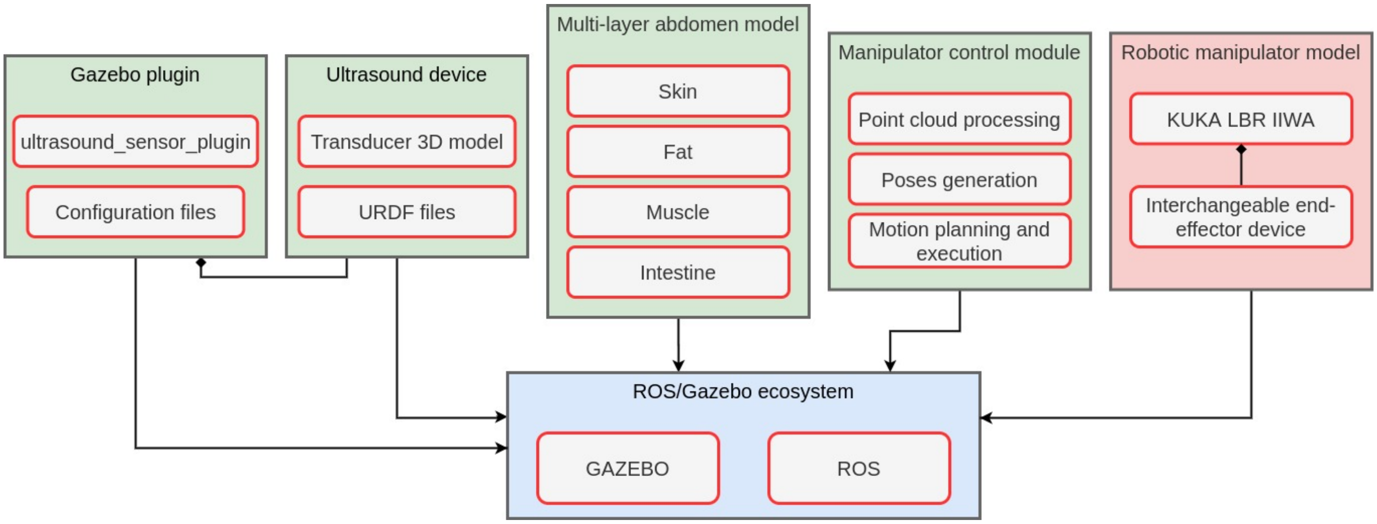

Fig. 1: Overview of ultrasound sensor package architecture. The system is composed of three components: ultrasound device, multi-layer abdomen model, and manipulator control module. The robotic manipulator model block consists of KUKA LBR IIWA but can be changed to another ROS-based manipulator model.

The developed *ultrasound_sensor_plugin* extension interacts with Gazebo engine and ROS subsystems for configuring and running the ultrasound imaging system. Once the virtual environment including the human abdomen model and the manipulator model equipped with the ultrasound device is loaded in Gazebo, the following steps are performed:

1) Processing of the abdomen model properties: density and propagation speed.
2) Processing of the transducer model properties: acoustic sound wave speed.
3) Calculating the acoustic impedance between two tissue mediums.
4) Calculating the intensity reflection coefficient.
5) Calculating the intensity transmission coefficient.

Acoustic impedance (Z) is a physical property of tissue. It describes how much resistance an ultrasound beam encounters as it passes through a tissue. Acoustic impedance is commonly used in determining the transmission and reflection at the boundary of two materials having different impedances.

Acoustic impedance depends on:

- density of a tissue (D, in kg/m^3)
- speed of the sound wave in the tissue (C, in m/s)

where density and propagation speed are related by:

$$Z = D * C \tag{1}$$

When an ultrasound wave travels from one medium to another with different impedance, part of the wave is reflected from the medium boundary. The rest of the wave is transmitted into the second medium. The process of reflection and transmision of ultrasound is shown is Fig. 5.

Reflected intensity (I_r) shows how much sound energy is reflected back. Can be calculated as:

$$I_r = (Z_2 - Z_1)^2 \tag{2}$$

where Z_1 and Z_2 are acoustic impedances of two tissue mediums making the boundary.

Incident intensity (I_i) shows how much sound energy could be transmitted through the two media:

$$I_i = (Z_1 + Z_1)^2 \tag{3}$$

Intensity reflection coefficient (R) is defined as the ratio of the intensity of the reflected wave relative to the transmitted wave. This statement can be written mathematically as:

$$R = I_r^2 / I_i^2 \tag{4}$$

A reflection coefficient of 0 (corresponding to total transmission and no reflection) occurs when the acoustic impedances of the two media are the same.

Intensity transmission coefficient (T) is defined as the ratio of the intensity of the transmitted wave relative to the reflected wave:

$$T = 1 - R \tag{5}$$

The *ultrasound_sensor_plugin* module extends the SDF format specification [23] used in World files for simulating virtual environments by defining new XML tags. The corresponding description of tissue medium in a World file is shown in Listing 1. The detailed description of each tissue parameter is given in Table I. **M** denotes mandatory parameters, **O** - optional.

Listing 1: A description of the abdomen tissue model structure.

```
<link name="tissue_name">
 <density>D</density>
 <wave_speed>C</wave_speed>
 <impedance>Z</impedance>
 <reflection>R</reflection>
</link>
```

TABLE I: Explanation of abdomen tissue parameters.

Parameter	Type	Description
D	M	Density of an abdomen tissue. Measured in kg/m^3.
C	M	Acoustic velocity in medium. Measured in m/s.
Z	O	Acoustic impedance. Measured in $kg/(m^2 * s)$.
R	O	Intensity reflection coefficient. In range [0.0...1.0].

The image formed by ultrasound data is made by tracking reflections and mapping the intensity of the reflected sound waves in a two-dimensional plane. The two-dimensional plane is a grayscale image where colors are shades of gray. Each pixel is stored as an 8-bit integer giving 256 possible different shades of gray from black (0) to white (255). A relative gray pixel value is assigned based on the intensity reflection of the returning signal. The higher number of the returning wave indicates the brighter area of the image. If the returned echo is relative small, then a darker pixel value will be assigned. Example of ultrasound imaging of the human heart is presented in Fig. 6.

In our package, the ultrasound sensor's imaging component is implemented as follows:

- *A piezoelectric element:* An RGB camera mounted to the transducer model is used to image each tissue. Transducer lens parameters description is shown in Listing 2. Parameters could be mandatory (M) or optional (O), which are described in details in Table II. *energy_density* and *frequency* parameters are not used in the current plugin implementation.
- *3D Mesh model control:* A special *model_links_manager* module is written and incorporated into *ultrasound_sensor_plugin* for configuring and controlling the human abdomen model: tissues (links), textures, parameters, etc. For example, to imitate wave emission through each tissue, *model_links_manager* performs showing the following and hiding the previous links.
- *Ultrasound imaging:* Once scanning tissues is done, an image processing module is handling tissue images received. It applies the intensity reflection coefficient to

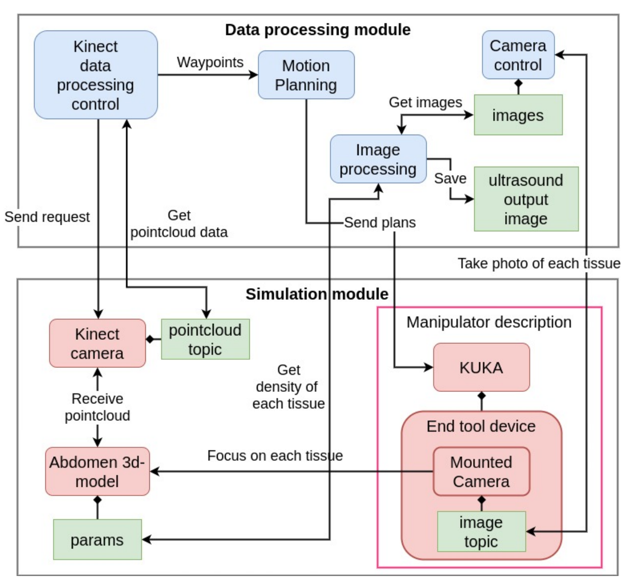

Fig. 2: Ultrasound sensor simulation in Gazebo.

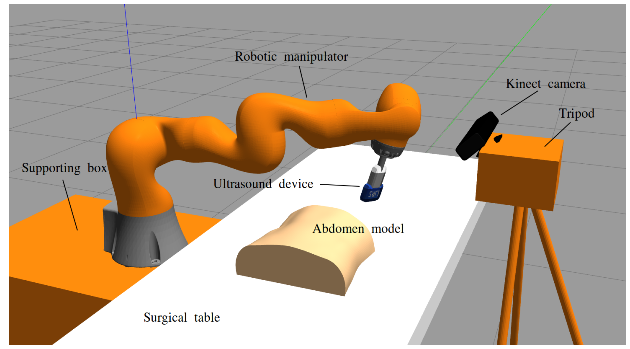

Fig. 3: A virtual environment in the Gazebo simulator.

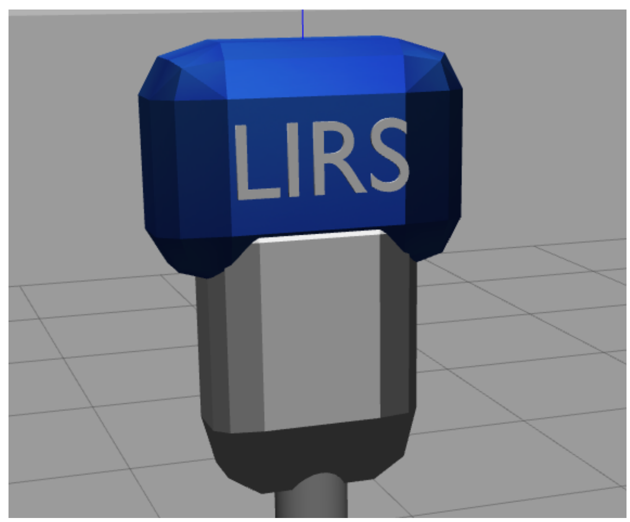

Fig. 4: A 3D model of the medical transducer.

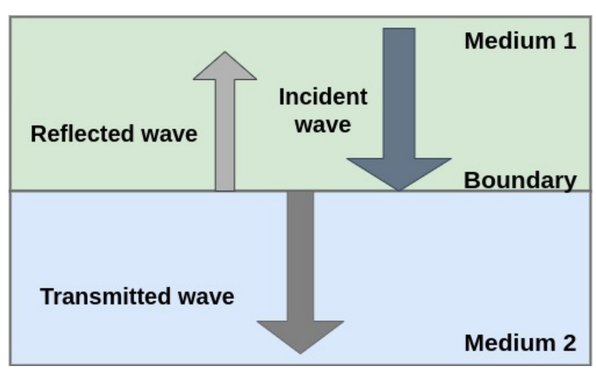

Fig. 5: Reflection and transmission waves movements between two mediums.

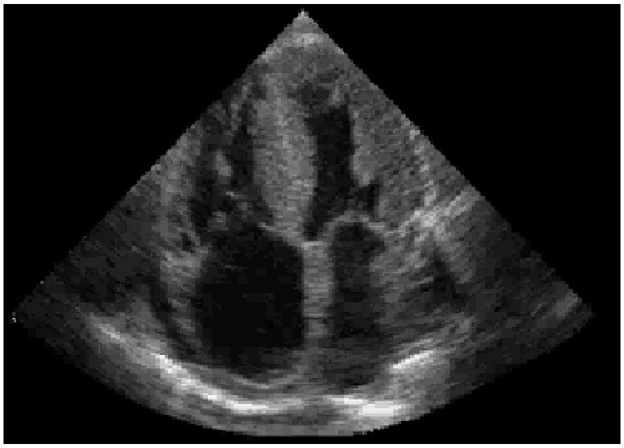

Fig. 6: An ultrasound image of the heart. White color encodes high reflection intensity. Black pixels show that the incident wave was transmitted fully through tissues. The image is borrowed from **sunshineanimalhospital.org**.

images by normalizing the value in the range [0...255] and generating a special image mask layout. This technique allows assigning shades of gray pixel values based on the intensity of the returning echo waves (Fig. 7). OpenCV library [24] was used for image processing.

Listing 2: A description of the transducer model structure.

```
<transducer name="transducer_name">
 <wave_speed>S</wave_speed>
 <energy_density>E</energy_density>
 <frequency>F</frequency>
</transducer>
```

TABLE II: Explanation of transducer device parameters.

Parameter	Type	Description
S	M	Ultrasound transducer velocities. Measured in m/s.
E	O	Ultrasound energy density. Measured in W/cm^3.
F	O	Frequency of wave affecting wavelengths. Measured in MHz.

C. Abdomen model

In order to emulate ultrasound in Gazebo, a complex multi-layer abdomen 3D model was modeled. It consists of fat, muscle, and intestine tissue layers 8. Each human tissue or organ is implemented as a model link defining in a World file. Blender [25]) was used as a third-party software solution for modelling and texturing abdomen layers. An example of an intestine 3D model in the simulation is presented in Fig. 9.

IV. Conclusions

This paper presented the software package for ultrasound sensor modeling in the Gazebo simulator. The package allows simulating ultrasound imaging process using the special Gazebo plugin. The ultrasound transducer device is based

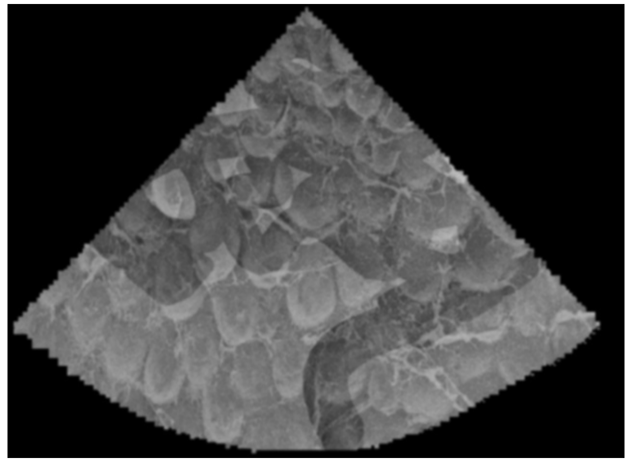

Fig. 7: An ultrasound image of the abdomen model in Gazebo. White areas show the higher density (fat), black regions are the lower density (muscle).

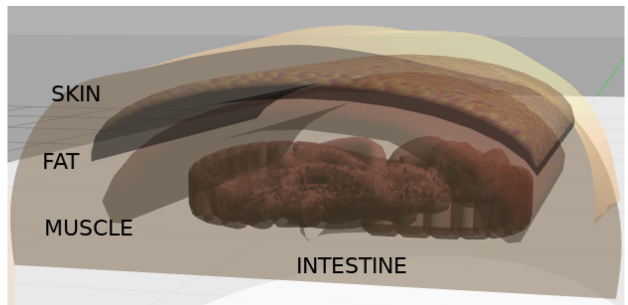

Fig. 8: A multi-layer abdomen model in the Gazebo simulation. Each layer has its shape, physical parameters, and texture.

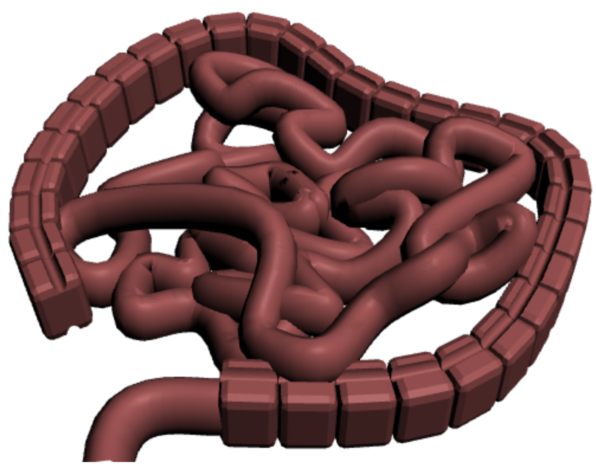

Fig. 9: A simplified intestine 3D model.

on KUKA IIWA LBR, but can easily be adapted for other ROS-based manipulator models. The developed multi-layer 3D abdomen model including fat, muscle, and intestine. The plugin utilizes data from tissues to compute the intensity reflection coefficient and produce an ultrasound grayscale view. The developed ultrasound sensor was successfully tested by simulating abdominal ultrasound imaging and was able to provide visualizing the abdomen internals for further diagnostics.

As a part of our future work, it is planned to improve the ultrasound imaging system by using transducer *energy_density* and *frequency* parameters and extend the abdomen model by remodeling existing links and adding new intermediate layers such as *connective tissues* and *peritoneum* in ROS/Gazebo.

Acknowledgment

The reported study was funded by the Russian Foundation for Basic Research (RFBR), project number 18-48-160037.

References

[1] M. Strydom, A. Banach, L. Wu, A. Jaiprakash, R. Crawford, and J. Roberts, "Anatomical joint measurement with application to medical robotics," *IEEE Access*, vol. 8, pp. 118 510–118 524, 2020.

[2] E. Magid, A. Zakiev, T. Tsoy, R. Lavrenov, and A. Rizvanov, "Automating pandemic mitigation," *Advanced Robotics*, pp. 1–18, 2021. [Online]. Available: https://doi.org/10.1080/01691864.2021.1905059

[3] J. Troccaz, G. Dagnino, and G.-Z. Yang, "Frontiers of medical robotics: from concept to systems to clinical translation," *Annual review of biomedical engineering*, vol. 21, pp. 193–218, 2019.

[4] G.-Z. Yang, J. Cambias, K. Cleary, E. Daimler, J. Drake, P. E. Dupont, N. Hata, P. Kazanzides, S. Martel, R. V. Patel *et al.*, "Medical robotics—regulatory, ethical, and legal considerations for increasing levels of autonomy," *Science Robotics*, vol. 2, no. 4, p. 8638, 2017.

[5] J. Hu, Y. Sun, G. Li, G. Jiang, and B. Tao, "Probability analysis for grasp planning facing the field of medical robotics," *Measurement*, vol. 141, pp. 227–234, 2019.

[6] R. A. Gondokaryono and A. Agrawal, "An approach to modeling closed-loop kinematic chain mechanisms, applied to simulations of the da vinci surgical system," *Acta Polytechnica Hungarica*, vol. 16, no. 8, 2019.

[7] M. Karnam, R. Parini, M. Eugster, P. Cattin, G. Rauter, and N. Gerig, "An intuitive interface for null space visualization and control of redundant surgical robots," *Proceedings on Automation in Medical Engineering*, vol. 1, no. 1, pp. 002–002, 2020.

[8] G. T. Clement, J. Sun, T. Giesecke, and K. Hynynen, "A hemisphere array for non-invasive ultrasound brain therapy and surgery," *Physics in Medicine & Biology*, vol. 45, no. 12, p. 3707, 2000.

[9] B. Fisher and S. Anderson, "Conservative surgery for the management of invasive and noninvasive carcinoma of the breast: Nsabp trials," *World journal of surgery*, vol. 18, no. 1, pp. 63–69, 1994.

[10] C. L. Moore and J. A. Copel, "Point-of-care ultrasonography," *New England Journal of Medicine*, vol. 364, no. 8, pp. 749–757, 2011.

[11] Q.-Y. Peng, X.-T. Wang, L.-N. Zhang, C. C. C. U. S. Group *et al.*, "Findings of lung ultrasonography of novel corona virus pneumonia during the 2019–2020 epidemic," *Intensive care medicine*, p. 1, 2020.

[12] Y. Y. Greenstein, R. Littauer, M. Narasimhan, P. H. Mayo, and S. J. Koenig, "Effectiveness of a critical care ultrasonography course," *Chest*, vol. 151, no. 1, pp. 34–40, 2017.

[13] R. Monfaredi, E. Wilson, B. A. koutenaei, B. Labrecque, K. Leroy, J. Goldie, E. Louis, D. Swerdlow, and K. Cleary, "Robot-assisted ultrasound imaging: Overview and development of a parallel telerobotic system," *Minimally Invasive Therapy & Allied Technologies*, vol. 24, no. 1, pp. 54–62, 2015.

[14] H. Li, W. Liu, K. Wang, K. Kawashima, and E. Magid, "A cable-pulley transmission mechanism for surgical robot with backdrivable capability," *Robotics and Computer-Integrated Manufacturing*, vol. 49, pp. 328–334, 2018.

[15] A. M. Priester, S. Natarajan, and M. O. Culjat, "Robotic ultrasound systems in medicine," *IEEE Transactions on Ultrasonics, Ferroelectrics, and Frequency Control*, vol. 60, no. 3, pp. 507–523, 2013.

[16] M.-A. Janvier, L.-G. Durand, M.-H. R. Cardinal, I. Renaud, B. Chayer, P. Bigras, J. De Guise, G. Soulez, and G. Cloutier, "Performance evaluation of a medical robotic 3d-ultrasound imaging system," *Medical image analysis*, vol. 12, no. 3, pp. 275–290, 2008.

[17] S. Wang, J. Housden, Y. Noh, D. Singh, A. Singh, E. Skelton, J. Matthew, C. Tan, J. Back, L. Lindenroth *et al.*, "Robotic-assisted ultrasound for fetal imaging: evolution from single-arm to dual-arm system," in *Annual Conference Towards Autonomous Robotic Systems*. Springer, 2019, pp. 27–38.

[18] R. O. Lavrenov, E. A. Magid, F. Matsuno, M. M. Svinin, and J. Suthakorn, "Development and implementation of spline-based path planning algorithm in ros/gazebo environment," *Trudy SPIIRAN*, vol. 18, no. 1, pp. 57–84, 2019.

[19] S. Chitta, E. Marder-Eppstein, W. Meeussen, V. Pradeep, A. R. Tsouroukdissian, J. Bohren, D. Coleman, B. Magyar, G. Raiola, M. Lüdtke *et al.*, "ros_control: A generic and simple control framework for ros," *The Journal of Open Source Software*, vol. 2, no. 20, pp. 456–456, 2017.

[20] A. Shafikov, T. Tsoy, R. Lavrenov, N. chiefermeier Mach, E. Maslak, E. Magid, and L. Hongbing, "Medical palpation autonomous robotic system modeling and simulation in ros/gazebo," *Proceedings of 13th International Conference on Developments in eSystems (DESE)*, 2020.

[21] R. B. Rusu and S. Cousins, "3d is here: Point cloud library (pcl)," in *2011 IEEE international conference on robotics and automation*. IEEE, 2011, pp. 1–4.

[22] A. Shafikov, A. Sagitov, H. Li, N. Schiefermeier-Mach, and E. Magid, "Robotic palpation modeling for kuka lbr iiwa using gazebo simulator," *Proceedings of International Conference on Artificial Life and Robotics*, vol. 25, pp. 436–439, 01 2020.

[23] W. Yao, W. Dai, J. Xiao, H. Lu, and Z. Zheng, "A simulation system based on ROS and Gazebo for Robocup middle size league," in *Iinternational Conference On Robotics And Biomimetics (ROBIO)*. IEEE, 2015, pp. 54–59.

[24] G. Bradski and A. Kaehler, "Opencv," *Dr. Dobb's journal of software tools*, vol. 3, 2000.

[25] A. Baglivo, F. D. Ponti, D. De Luca, A. Guidazzoli, M. C. Liguori, and B. Fanini, "X3d/x3dom, blender game engine and osg4web: open source visualisation for cultural heritage environments," in *2013 Digital Heritage International Congress (DigitalHeritage)*, vol. 2. IEEE, 2013, pp. 711–718.